Lasers in Manufacturing Conference 2023

Plasma-assisted laser cutting of stainless steel: An analysis of a first prototypical setup

Franz Urlau[a,*], Achim Mahrle[b], Sebastian Manzke[a], Moritz Krümmer[a], Christoph Leyens[a,b], Uwe Füssel[a]

[a] *Technische Universität Dresden, Institute of Materials Science, PO-Box, 01062 Dresden, Germany*
[b] *Fraunhofer Institute for Material and Beam Technology IWS, Winterbegstraße 28, 01277 Dresden, Germany*

Abstract

A new concept of solid-state laser fusion cutting is presented. The suggested approach applies a non-transferred hot argon plasma jet as auxiliary gas instead of the commonly used cold high-pressure nitrogen jet. Cutting experiments on 6 mm thick AISI 304 stainless steel samples were performed for both variants. Based on a two-level factorial design, the influence of geometrical and process parameters on the cutting performance, the kerf geometry and the cut edge quality was analyzed. With the hot plasma jet, the delivery pressure and the nozzle diameter of the auxiliary gas supply could be drastically reduced while maintaining a good cut edge quality compared to cutting with the cold high-pressure gas jet. As a result, a more than tenfold decrease in gas consumption was achieved.

Keywords: fibre laser cutting; plasma-assisted laser cutting; plasma jet; stainless steel

1. Introduction

Laser beam cutting applies a focused laser beam in combination with a gas jet to melt and blow out material from a cutting zone. Designed cutting heads usually arrange both tools in a coaxial way. Because of a continuous movement of the cutting head along the desired cut contour, a generated cut kerf eventually separates the part to be manufactured from the base material. The applied gas type determines the process variant and the particular parameter settings: Reactive laser cutting at relatively low gas pressures in a range between 1 and 5 bar uses reactive oxygen as a cutting gas while fusion cutting at high gas pressures up to 20 or even 30 bar applies nitrogen. Industrial users do preferably apply reactive laser cutting for mild steel sheet cutting and the main application domain of laser fusion cutting is cutting stainless steel samples. Reactive laser cutting is a very established technology and offers a high-quality cutting performance for different laser sources, including CO_2 lasers, and solid-state lasers such as fiber and disk lasers. In contrast, the laser type has

a crucial influence on the cutting performance in fusion cutting of stainless steel. Solid-state laser sources with an emission wavelength of about 1 µm outperform CO_2 laser sources with a wavelength of 10.6 µm in thin-section cutting up to sheet thicknesses of 4 mm with respect to achievable cutting speeds but do not reach the bright cut edge quality of the CO_2 laser in cutting thicker materials. A lot of recent work was dedicated to explain those differences including aspects of a wavelength-dependent absorptivity and changed melt flow characteristics. In addition, researchers proposed different technical solution strategies to improve the performance of cutting thicker steel sheets, e.g. by dynamic and static beam shaping methods, beam superposition and adapted nozzle concepts. A rather new approach aims to replace the cold high-pressurized nitrogen gas jet by a hot plasma jet (Mahrle et al., 2018). Steen (1979, 1980) pursued a similar idea in his work on laser-arc processing but in contrast to those early investigations with a conventional transferred electric arc, the proposed current approach suggests a non-transferred plasma jet that allows for a separation of the melting and ejection process as in conventional laser fusion cutting.

2. Theoretical considerations

The idea of combining a laser beam and a plasma jet for separating metals initially came up from a technological review of laser and plasma cutting and a comparison of the specific advantages and drawbacks that each of these technologies can offer. At the end, the question aroused if a synergistic combination of both variants would be possible to put forward the individual advantages but to compensate the drawbacks as it was already demonstrated in the field of hybrid laser-arc processing for welding applications (e.g. Mahrle and Beyer,2006). Concerning the practical experience gained from the work by Kamalu(1981), it became obvious that a successful combination inevitably needs a decoupling of energy and momentum transfer by applying a non-transferred Direct Current (DC) arc. Because the energy transfer from an electric arc to a work-piece or material is mainly determined by energy conversions within the transition region of the anodic sheath, the energy transfer of a non-transferred arc to a work-piece is minimized and the laser beam alone acts as primary energy source as in conventional laser cutting. Additional theoretical considerations show that an improved momentum transfer is highly anticipated in case of the plasma jet. These expectations relate to the inherent changes in dynamic viscosity and density as a function of temperature. A first rough estimation of these properties assumes argon as a plasma gas with an averaged (and relatively low) plasma temperature $T_{\mathrm{Ar}} = 5000\ \mathrm{K}$. The dynamic viscosity $\eta_{\mathrm{Ar},5000\mathrm{K}}$ follows from the well-known Sutherland-Model to

$$\eta_{\mathrm{Ar},5000\mathrm{K}} = \eta_{0,\mathrm{Ar}} \cdot \left(\frac{T_{0,\mathrm{Ar}} + C_{\mathrm{Ar}}}{T + C_{\mathrm{Ar}}}\right) \cdot \left(\frac{T}{T_{0,\mathrm{Ar}}}\right)^{3/2} = 1.4 \times 10^{-4}\mathrm{Pa\ s} \qquad (1)$$

with $\eta_{0,Ar} = 2.1 \times 10^{-5}\mathrm{Pa\ s}$, $T_{0,Ar} = 273\ \mathrm{K}$ and $C_{Ar} = 165\ \mathrm{K}$ (White, 1991). The calculated value of $\eta_{\mathrm{Ar},5000\mathrm{K}}$ is very close to the results of the detailed calculations of Murphy and Arundell (1994) that show a further increase of viscosity up to $2.7 \times 10^{-4}\mathrm{Pa\ s}$ for plasma temperatures about $10000\ \mathrm{K}$, whereas for higher temperatures the viscosity decreases again. In comparison, the viscosity of nitrogen at $T_{\mathrm{N2}} = 300\ \mathrm{K}$ amounts to $\eta_{N2,300K} = 1.8 \times 10^{-5}\mathrm{Pa\ s}$, which gives – relating this value to $\eta_{\mathrm{Ar},5000\mathrm{K}}$ – a ratio of 7.8, i.e. the viscosity of the plasma is almost one order of magnitude higher than that of the cold gas. A higher viscosity causes higher shear stresses at the interface between gas and molten material and is therefore expected to facilitate the blow out of the molten material. In addition, the viscosity has a vital influence on the flow state of the gas. An assumed reference gas pressure of $P_{\mathrm{ref}} = 5\ \mathrm{bar} = 5 \times 10^5\mathrm{Pa}$ that corresponds to a lower limit in conventional laser fusion cutting but is very likely an upper limit in plasma-assisted laser cutting allows for an estimation of characteristic values of the Reynolds number. With the specific gas constants of $R_{N2} = 296.8\ \mathrm{J/(kg\ K)}$ and $R_{Ar} = 208.1\ \mathrm{J/(kg\ K)}$, gas densities follow from the state equation of ideal gases to

$\rho_{\mathrm{N2,300K}} = 5.615\ \mathrm{kg/m^3}$ and $\rho_{\mathrm{Ar,5000K}} = 0.481\ \mathrm{kg/m^3}$ for the assumed reference pressure. Furthermore, characteristic flow velocities are assumed to be in the order of the speed of sound which are given by $u_{\mathrm{S,N2,300K}} = \sqrt{\kappa_{\mathrm{N2}} \cdot R_{\mathrm{N2}} \cdot T_{\mathrm{N2}}} = 353.1\ \mathrm{m/s}$ and $u_{\mathrm{S,Ar,5000K}} = 1318.2\ \mathrm{m/s}$ for $\kappa_{N2} = 1.4$ and $\kappa_{Ar} = 1.67$. Corresponding Reynolds numbers for a characteristic length of $l_{\mathrm{ch}} = 1 \times 10^{-3}\mathrm{m}$ as upper limit of the cut kerf widths are:

$$Re_{N2,300K} = \frac{\rho_{N2,300K} \cdot u_{S,N2,300K} \cdot l_{ch}}{\eta_{N2,300K}} = 110148 \qquad (2)$$

$$Re_{Ar,5000K} = \frac{\rho_{Ar,5000K} \cdot u_{S,Ar,5000K} \cdot l_{ch}}{\eta_{Ar,5000K}} = 4529 \qquad (3)$$

This result allows for the conclusion that the plasma flow through the cut kerf has much lower grades of turbulence than the cold nitrogen flow and is even likely to reach a laminar flow regime if the real pressure values drop below the assumed reference pressure of $P_{\mathrm{ref}} = 5 \times 10^5\mathrm{Pa}$. In addition to these prospects of higher shear stresses and lowered turbulence grades, also the gas consumption is assumed to be significantly lowered because of a proportionality $\dot{m}_{Gas} \sim T_{Gas}^{-1/2}$ for the mass flow rate of a gas that flows out from a conical nozzle at sonic speed.

The performed theoretical analysis motivated the built-up of an appropriate setup for corresponding practical investigations of a plasma-assisted laser cutting process. A first study aimed to compare the characteristics of cold gas and plasma gas cutting under comparable processing conditions of an inclined serial gas supply.

3. Experimental setup & methods

The experimental setup consists of a perpendicular laser beam and a mount, which holds the non-coaxially inclined gas supply. This can be either an aluminum tube with a commercially available nozzle of a conventional laser cutting head for cold gas cutting or a plasma torch, developed for this study (Manzke et al., 2023). Fig. 1 (left) depicts the variant for plasma-assisted cutting with the plasma torch as auxiliary gas supply.

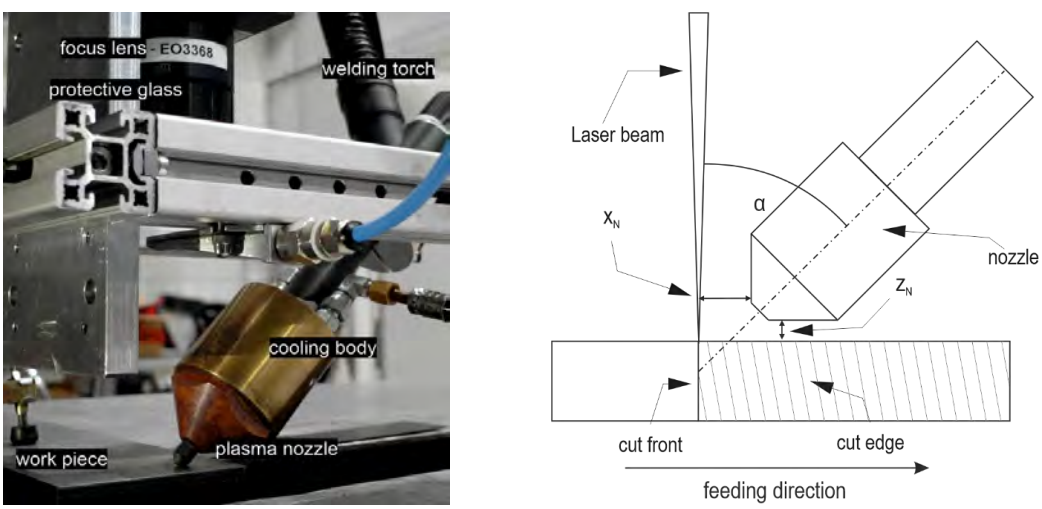

Fig. 1. (left): Picture of the experimental setup with the applied plasma torch; (right): schematics of the setup with the principal geometrical degrees of freedom

Fig. 1 (right) additionally illustrates the three principal geometrical degrees of freedom of the setup: The gas supply can be moved along the feeding direction of the metal sheet and has therefore an adjustable distance x_N to the laser beam. Furthermore, the distance between the nozzle and the sheet can be varied (z_N). The angle α between the plasma jet and the laser beam is adjustable between 35° und 45°. The laser beam has to be kept in a horizontal distance to the plasma torch as well, to ensure that the beam does not graze the plasma torch. In addition, the horizontal distance and the inclination angle of the nozzle define the point of impingement of the anticipated gas jet axis on the cutting front. As a laser source, the fiber laser IPG YLS4000-S2T with a fiber diameter of 100 µm is used. The beam is collimated by a 100 mm lens and focussed by a lens with a focal length of 200 mm. Thus, the beam waist diameter in the focal plane is 200 µm. Cutting experiments were conducted on 6 mm thick AISI 304 stainless steel.

The parameters in Table 1 where kept constant for all conducted experiments. They were determined in preliminary tests and ensure evaluable cutting results in a wide parameter range of selected changeable parameters. The inclination of the gas supply was already researched by several authors using non-coaxial cutting setups. Hsu (1992) recommended an angle of 20° to 45°between laser beam and nozzle axis. Brandt and Settles (1997) narrowed the range of preferable angles to 35° to 40° and made the suggestion that the impinging point of the gas jet should be inside the cut kerf below the upper sheet surface. Ilavarasan & Molian (1995) found the best angle to be 40° and reinforced the argument that the impinging point should be inside the cut kerf preferably at a depth below the upper surface corresponding to 30% of the sheet thickness of the material being cut. In this study an angle α = 45° was used to ensure a minimal distance between the laser beam and the nozzle exit for the plasam torch.

Table 1: Fixed parameters of the experimental trials.

Fixed Parameter	Value
Laser Power P_L	4 kW
Cut Velocity v_C	4 m/min
Vertical Distance z_N	0.7 mm
Focus Position z_f	-3 mm
Inclination of Gas Supply α	45°

The ability to remove molten material from the cut kerf rises with increasing shear forces exerted by the auxiliary gas and the stagnation pressure inside the cut kerf, as Vicanek and Simon (1987) showed. For cold gas cutting, these effects are determined by the *pressure p* and by the *nozzle diameter* d_N, the latter by its strong influence on the flow rate through the nozzle. For hot gas cutting, the electric *current I* in the plasma torch is added as a parameter influencing the temperature and accelaration of the auxiliary gas. To evaluate the significance of the influence of the above-mentioned parameters as well as the *horizontal distance* x_N as geometrical parameter, a 2-level-factorial scheme following the rules of Design of Experiment (DoE) was performed.

The lower and upper values of the limits where defined after preliminary tests to ensure a wide range of cutting qualities, while assuring the ability to cut through the material for all addressed factor-factor combinations. The geometrical factors x_N and d_N have the same limits for cold gas as well as hot gas cutting, while the limits for pressure p differ distinctly. The high values for the horizontal distance relative to the vertical distance of the nozzle ensure that the impinging point of the gas jet is inside the cut kerf. Table 2 gives an overview about the limits of the experimental design, which also addresses the center points of the parameter ranges to account for a possible curvature in the dependencies of the respective parameters.

Table 2: Factors Limits of 2-level factorial design for cold gas cutting and plasma-assisted cutting

	Cold gas cutting		Hot gas cutting	
Factor	low limit	high limit	low limit	high limit
Horizontal Distance x_N	2.0 mm	3.5 mm	2.0 mm	3.5 mm
Nozzle Diameter d_N	1.5 mm	2.1 mm	1.5 mm	2.1 mm
Pressure p	0.6 MPa	1.4 MPa	0.2 MPa	0.4 MPa
Current I			75 A	125 A

Quantifiable as well as unquantifiable responses of the cutting experiments serve as evaluation criteria of the cutting quality. Microscopy allowed for measurements of the top and bottom kerf widths. The cut edge roughness was measured with the Profilometer *Hommel-Etamic W20* (Jenoptik AG) according to DIN EN ISO 4288. The dross height at the bottom of the cut kerf is derived from microscopic images and evaluated as follows: Based on the specification of roughness measurement according to DIN EN ISO 4288, the cut length is divided into 5 parts. The arithmetic mean dross height was calculated from the five respective measured maximum dross heights. Possible oxidation on the cut edge was visually evaluated by its appearance. The existence of different temper colors as far as a black layer on the cut edge is a sign for several stages of oxidation.

4. Results

4.1. Kerf width

The upper cut kerf width strongly correlates to the diameter of the laser beam at the upper surface. Therefore, the kerf width primarily depends on the caustic of the laser beam and the focus position relative to the upper sheet surface. As the optical setup and the focal position is constant for all experiments, there is no significant variance in the upper kerf width. The mean upper kerf width is about 430 µm for all executed experiments, including cold and hot gas configurations. Besides the focal position, the lower kerf width also depends on the flow behavior of the molten material. Re-solidified material near the lower sheet surface can narrow the kerf width. The gas flow characteristics, as well as the physical properties of the gas, e.g. the viscosity, influence the shear forces and thereby the ability to drag molten material in direction of the lower end of the kerf. Within the separate experimental designs for the cold and the hot gas, no parameter on its own can be statistically identified that significantly influences the lower kerf width but it can be noted that there is an overall difference between the usage of cold gas and hot gas (plasma) as auxiliary medium. The mean lower kerf width for material cut with cold auxiliary gas is about 50 µm lower as for the same material cut with hot gas as depicted in Fig. 2. That result allows for the conclusion that the plasma jet is either capable to melt some additional amounts of material and/or it blows the melt more efficiently out of the cut kerf. However, the difference is small with some overlap within the ranges of the standard deviation of the cold and hot gas data values. This is an indication that a possible additional heat input by the hot plasma gas and/or the cooling effect of the cold gas are playing no vital roles for the cut kerf formation. The tendency to generate more perpendicular cut edges with ratios of upper and lower kerf width close to unity in case of plasma-assisted laser cutting is even a desirable effect.

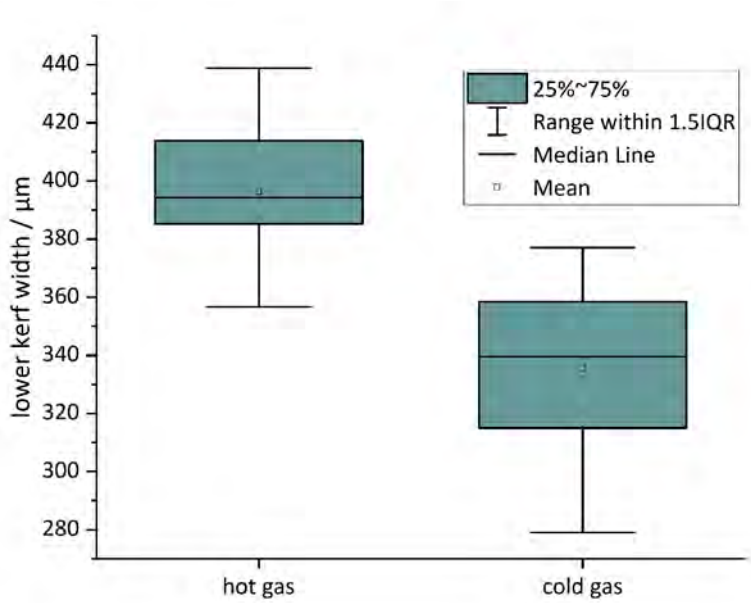

Fig.2. Box plot of lower kerf width

4.2. Dross height

The ability to blow out the molten material in an efficient way manifests itself particularly in the suppression of adhering dross at the lower cut kerf. The dross height is an important quality parameter in laser cutting. Different kinds of dross can be commonly distinguished in laser cutting, correlating to the cutting velocity and focal position of the laser beam in the work piece (Pacher et al, 2020), Mahrle et al., 2021). Under the conditions of this study, the most vital parameters for dross suppression in cold gas cutting were the gas pressure and the nozzle diameter: Increasing these parameters leads to a reduced dross height as depicted in Figure 3 (left). A nearly dross free cut (dross height: 178µm) is possible with exception of a few occasional droplets at the lower cut edge for cutting with the upper levels of nozzle diameter (2.1 mm) and gas pressure (1.4 MPa).

For hot gas cutting, the dependencies are much more complex and the process generally shows a higher tendency to be accompanied by adherent dross. As with cold gas cutting, increasing the *pressure* leads to reduced dross heights. The same is true for raising the *electric current I* of the plasma source. However, and in contrast to the findings in cold gas cutting, the *nozzle diameter* shows an opposing dependency: The wide nozzle diameter leads to an increased dross height at the lower cut edge (see Figure 3 (right)). The minimal achievable dross height for hot gas cutting is 460 µm (d_N = 1.5 mm, p = 0.4 MPA, I = 75 A, x_N= 3.5 mm). Some severe oxidized droplets always remain on the lower cut edge. These few droplets determine the calculated dross height by contributing to the arithmetic mean, as the maximum dross height in their respective part of the cut edge. This discontinuity of the dross is not reliably represented by the chosen method for measuring the dross height.

Furthermore the position of the center points in the depicted diagram (Fig.3 (right) indicate some curvature, i.e. inherent nonlinearities, in the model, which cannot be resolved in this 2-level factorial design.

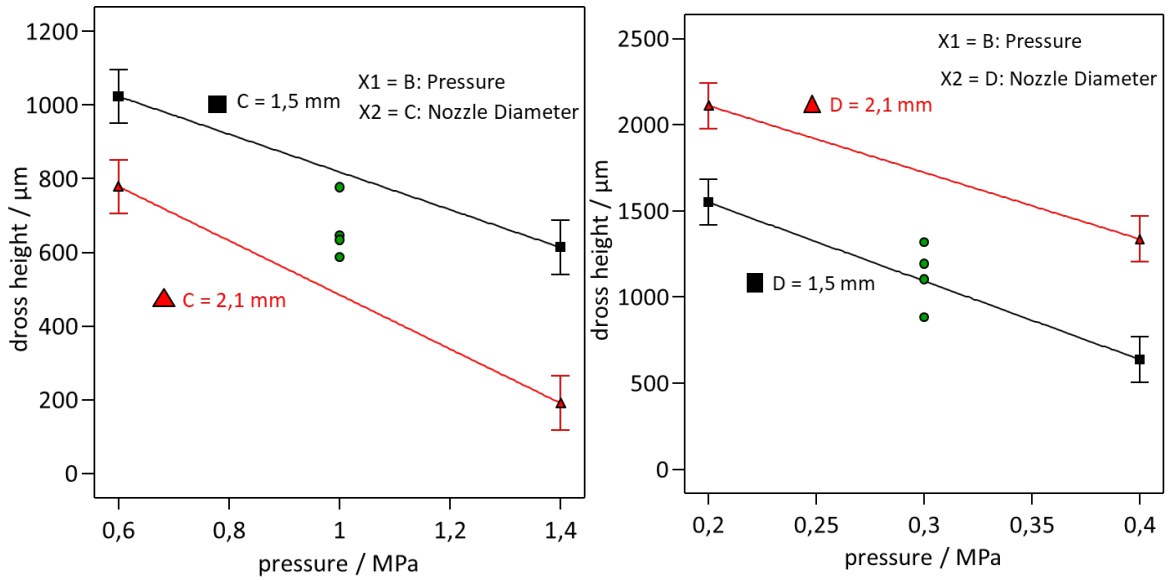

Fig. 3. Dross height as function of gas pressure and nozzle diameter for (left): cold gas cutting, (right) plasma-assisted laser cutting

4.3. Oxidation

Process-accompanying oxidation of the cut edge is only possible if oxygen is present in the cutting zone and the temperatures of the stainless steel samples are still high in a range of approximately > 600°C. After the laser beam passed a certain area along the cut contour the molten material rapidly cools down by heat conduction in the surrounding base material, properly supported by convective energy transfer to the cold gas jet. The usage of nitrogen as auxiliary gas prevents the oxidation in laser fusion cutting due to the absence of oxygen. However, in some cases of cold gas cutting, the oxidation was not fully prevented. The nozzle diameter and the pressure define the flow rate of the auxiliary gas. One could argue that a high flow rate is necessary to prevent oxidation by replacing the atmospheric oxygen from the cut kerf. However, this general conclusion is found to be not true in all cases. Fig. 4 depicts cut edges for different parameter configurations, on the left-hand-side sample NK3.04 with a nitrogen flow rate of $\dot{V}_{N2} = 179$ NLPM (normal litre per minute) (d_N = 1.5 mm, p = 1.4 MPa), and on the right-hand-side sample NK3.08 with a nitrogen flow rate of $\dot{V}_{N2} = 136$ NLPM (d_N = 2.1 mm, p = 0.6 MPa). Although sample NK3.08 was cut with a lower flow rate there is less oxidation apparent in comparison to NK3.04. The bigger nozzle diameter, used in trial NK3.08 is the vital parameter for preventing oxidation of the cut edges while the pressure seems to have a subordinate effect. Increasing the pressure can just reduce oxidation while using a constant nozzle diameter. A wide nozzle diameter ensures that the kerf is completely shielded from the surrounding atmosphere. On the other hand, it is anticipated that a small nozzle diameter allows the gas jet to suck parts of the surrounding atmosphere into the cut kerf, which can lead to oxidation of the cut edges.

Under the conditions of the current serial implementation of the laser cutting process, oxidation of the cut edge is a much more serious issue in the plasma-assisted variant. There was usually a multicolor appearance of temper colors on the cut edge – as shown by sample P3.14 in Fig. 5 (left) – especially in the upper and lower part of the cut edge. A black oxidation layer indicating a high thickness is primarily promoted for small nozzle diameters and larger horizontal distances between the laser beam and the nozzle (high level). Oxidation can

be reduced by using the wider nozzle diameter. However, at least at the margins of the cut edge there are still some amounts of surface oxidation visible, see sample P3.02 in Fig. 5 (right).

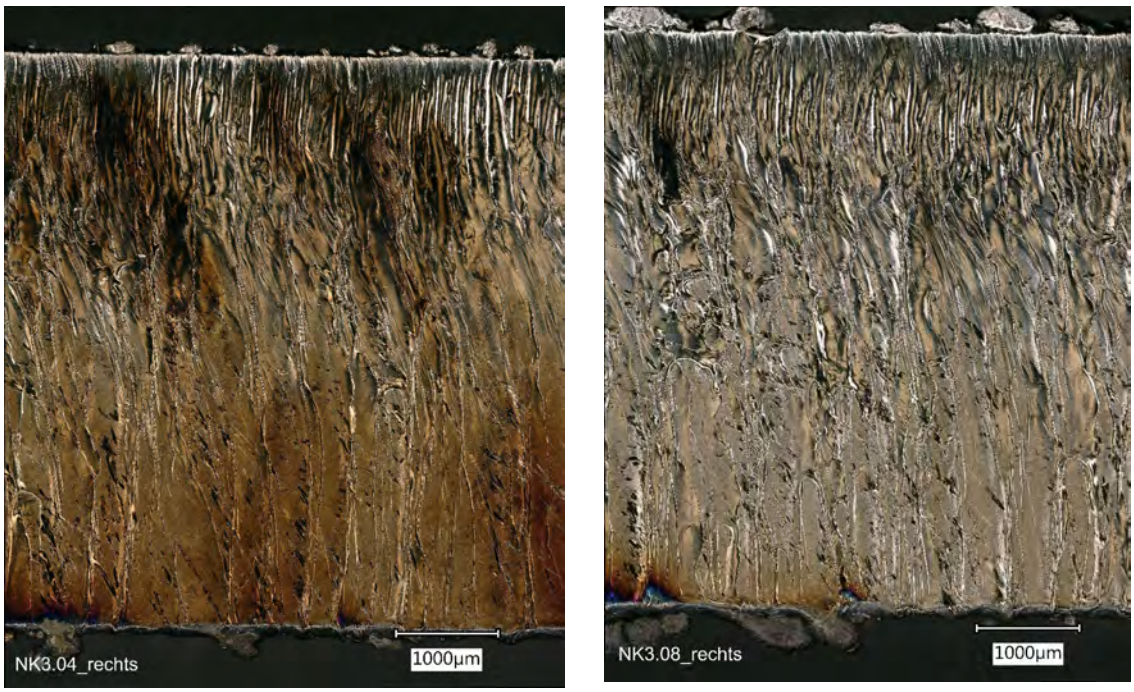

Fig. 4. cut edges of cold gas cut (left): NK3.04 (d_N = 1.5 mm, p = 1.4 MPa, x_N = 2 mm); (right): NK3.08 (d_N = 2.1 mm, p = 0.6 MPa, x_N = 2 mm)

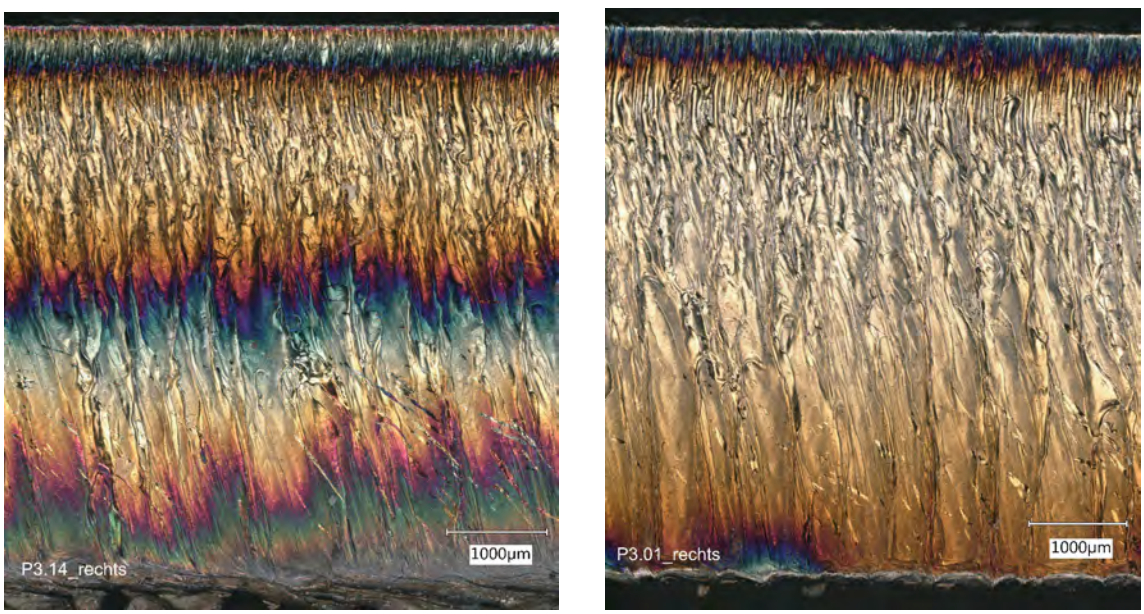

Fig. 5. cut edges of hot gas cut (left): P3.14 ((d_N = 1.5 mm, p = 0.2 MPa, I = 125 A, x_N = 2 mm); (right): P3.02 (d_N = 2.1 mm, p = 0.4 MPa, I = 125 A, x_N = 3.5 mm)

4.4. Roughness

The topography of the cut edges is comparable for all conducted cutting experiments. The striations, which are typical for laser cutting with solid-state lasers, are apparent for cold as well as hot gas cutting despite the large differences in the theoretical values of the Reynolds number as characteristic dimensionless quantity of the flow state of the gas (see Fig.4 and Fig. 5). The light inclination of the striations may derive from the non-coaxial impinging gas jet. Measured roughness values R_Z for cold gas cutting lie in a range of 47 µm to 63 µm with a mean value of R_Z = 53 µm and a standard deviation of 5.2 µm. For hot gas cutting the range of measured roughness values is between 47µm and 102 µm with a mean value of R_Z = 63 µm and a standard deviation of 14.2 µm. The higher range and standard deviation for hot gas cutting originates from two samples, which show distinct melt streams on the cut edge. All remaining samples have roughness values in a comparable range to cold gas cutting. Surprisingly, these measured roughness values do not show any statistically significant dependency on tested parameters and are in the same order of magnitude for cold as well as hot gas cutting.

4.5. Gas consumption

One pronounced benefit of plasma-assisted laser cutting is the significantly lowered gas consumption. A low dross height and the absence of oxidation could be assured for cold gas cutting at the respective high levels of pressure and nozzle diameter, i.e. for a pressure p = 1.4 MPa and a nozzle diameter of d_N = 2.1mm. This gives a corresponding gas flow rate of $\dot{V}_{N2}$ = 298 NLPM. The mean gas flow rate for plasma-assisted cutting is an order of magnitude lower and is in a range from $\dot{V}_{Ar}$ = 15 NLPM to $\dot{V}_{Ar}$ = 31 NLPM. The best cut quality with low dross height and minimized amounts of oxidation was achieved with d_N = 2.1 mm and p = 0.4 MPa giving rise to a corresponding flow rate of $\dot{V}_{Ar}$ = 31 NLPM, a tenth of the flow rate required in cold gas cutting

5. Discussion

A good cut edge quality is indicated by low dross heights and the absence of any oxidation on the cut edge. For cold gas cutting the necessary parameters to achieve a good quality cut are well known from standard laser fusion cutting with a coaxial arrangement of laser beam and gas jet. The principal tendencies could be also reproduced for the applied non-coaxial setup. A high pressure and a wide nozzle diameter promote the desired quality attributes. Increasing these parameters leads to an increased flow rate, which facilitates the blow out of the molten material. Hence, the dross height is minimized and oxidation is prevented. However, these parameters should also be limited to prevent an excess consumption of auxiliary gas.

For hot gas cutting, the dependencies are still inconclusive. In contrast to cold gas cutting, and under the conditions of the current experimental setup and design, it was found that the height of the adherent dross can be minimized by reducing the nozzle diameter. A possible explanation for this phenomenon could be the raised speed of sound at elevated temperatures as shown above. It is plausible to assume that the speed of sound is not reached during hot gas cutting. Schlieren images support this assumption, where no shock waves are apparent in the gas flow. Because of the subsonic speed the nozzle diameter has a distinct influence on the flow speed of the gas. The higher flow speed through the smaller nozzle (d_N=1.5mm) raises the exerted shear stress and hence the adherent dross height is reduced. However, the prevention of oxidation cannot be reliably achieved using a small nozzle diameter. The chrome oxides formed during cutting of stainless steel have a high melting temperature and viscosity. This can interfere with material blow out, which could be the reason for the overall higher dross heights in hot gas cutting. Besides that, the oxidation should be minimized in order to retain the inhibition of corrosion in the stainless steel. The opposing dependencies, regarding the reduction of dross and oxidation, hamper a clear definition of preferable parameters for hot gas laser cutting.

If the oxidation could be reduced through other measures, a smaller nozzle diameter would be preferable. This could for instance be achieved by creating a reducing atmosphere by adding a small amount of hydrogen to the auxiliary gas. Otherwise a wider nozzle diameter accompanied by a high current and pressure leads to a low dross height with a minimum of oxidation on the cut edge.

6. Summary and outlook

In this study a comparison was made between the conventional cold gas laser cutting and a new approach, the plasma-assisted laser cutting, based on a 2-level factorial design of experiment. It could be shown that laser cutting benefits from increasing the temperature of the auxiliary gas by remarkably reducing the gas consumption, while maintaining a low height of the adherent dross at the lower cut edge for particular parameter settings. However, the anticipated effects of the high viscosity and low density of the hot gas jet on the cut edge topography and the corresponding roughness could not be fully exploited with the current experimental setup. Especially, an unintended oxidation of the cut edge could not be avoided. Facing these challenges will be the objective of further studies, particularly by developing a coaxial setup of laser beam and auxiliary gas jet that will allow for shorter nozzle stand-off distances as in conventional laser fusion cutting.

Acknowledgement

This research was funded by the German Research Foundation DFG within the project “Entwicklung und Analyse des plasmaunterstützten Laserstrahlschmelzschneidens”, Contract No. LE 1373/72-1 and FU 307/20-1. This support is highly appreciated by the authors.

References

Brandt, A.D., Settles, G.S., 2012. Effect of nozzle orientation on the gas dynamics of inert-gas laser cutting of mild steel, Journal of Laser Applications, 9(269), 269-277.

Hsu, M.J., 1992. Analytical and experimental studies of advanced laser cutting techniques, Dissertation, Iowa State University, Department of Mechanical Engineering, Ames (Iowa), 1992.

Ilavarasan, P.M., Molian, P.A., 1995. Laser cutting of thick sectioned steels using gas flow impingement on the erosion front

Kamalu, J.N., 1981. Laser cutting of mild steel: Gas flow, arc augmentation and polarization effects, PhD Thesis, University of London, 1981.

Mahrle, A., Herwig, P., Hipp, D., Jäckel, S., Hertel, M., 2018. Verfahren und Vorrichtung zum plasmagestützten Laserstrahlschneiden – Apparatus for laser beam cutting and a method for laser beam cutting, Patent Application DE 10 2018 205 906 A1 (pending), 2018.

Mahrle, A., Borkmann, M., Pfohl, P., 2021. Factorial Analysis of Fiber Laser Fusion Cutting of AISI 304 Stainless Steel: Evaluation of Effects on Process Performance, Kerf Geometry and Cut Edge Roughness, Materials, Vol.14, No. 10, Published online: 19 May 2021

Mahrle, A., Beyer, E., 2006. Hybrid laser beam welding – Classification, characteristics, and applications, Journal of Laser Applications, 18(169), 169-180, 2006.

Manzke, S., Krümmer, M., Urlau, F., Mahrle, A., Füssel, U., Leyens, C., 2023. Numerical study of a plasma jet for plasma-assisted laser cutting, Welding in the World, Published online: 01 April 2023.

Murphy, A.B., Arundell, C.J.,1994. Transport coefficients of argon, nitrogen, oxygen, argon-nitrogen, and argon-oxygen plasmas, Plasma Chemistry and Plasma Processing, Vol. 14, No. 4, 451-490, 1994.

Pacher, M., Franceschetti, L., Strada, S.C., Tanelli, M., Savaresi, S.M., Previtali, B., 2020. Real-time continuous estimation of dross attachment in the laser cutting process based on process emission images, Journal of Laser Applications, Vol. 32, No. 4, 042016, 2020

Steen, W.M., 1979. Methods and apparatus for cutting and welding, U.S. Patent 4,167,662, September 11, 1979.

Steen, W.M., 1980. Arc augmented laser processing of materials, Journal of Applied Physics, 51(11), 5636-5641, 1980.

Vicanek, M., Simon, G. ,1987. Momentum and heat transfer of an inert gas jet to the melt in laser cutting, Journal of Physics D: Applied Physics, 20, 1191-1196, 1987.

White, F.M., 1991. Viscous Fluid Flow, 2nd edition, McGraw-Hill, 1991.